Riemannian Statistical Analysis of Cortical Geometry with Robustness to Partial Homology and Misalignment

Suyash P. Awate[1(✉)], Richard M. Leahy[2], and Anand A. Joshi[2]

[1] Computer Science and Engineering Department,
Indian Institute of Technology (IIT) Bombay, Mumbai, India
suyash@cse.iitb.ac.in
[2] Signal and Image Processing Institute (SIPI),
University of Southern California (USC), Los Angeles, USA

Abstract. Typical studies of the geometry of the cerebral cortical structure focus on either cortical folding or thickness. They rely on spatial normalization, but use cortical descriptors that are sensitive to misregistration arising from the well-known problems of partial homologies between subject brains and local optima in nonlinear registration. In contrast to these approaches, we propose a novel framework for studying the geometry of the *entire cortical sheet*, subsuming its folding and thickness characteristics. We propose a novel descriptor of local cortical geometry to increase robustness to partial homology and misregistration. The proposed descriptor lies on a Riemannian manifold, and we describe a method for hypothesis testing on manifolds for cross-sectional studies. Results on simulated and clinical data show the benefits of the proposed approach for detecting between-group differences with greater accuracy and consistency.

Keywords: Brain cortex · Folding · Thickness · Riemannian space · Hypothesis tests

1 Introduction and Related Work

Studies of cerebral cortical geometry can provide insights into development, aging, and disease progression. We propose a novel framework to study the geometry of the entire *cortical sheet*, subsuming its folding and thickness properties and modeling the complementary nature of these two attributes. Our histogram-based approach provides robustness to partial homologies and misregistration in detecting inter-cohort differences.

Typical cross-sectional cortical studies of thickness [6,10,18] or folding [16,21,22] first perform spatial normalization and then conduct hypothesis tests at every cortical location in the normalized space. However, it is difficult to find a

S.P. Awate—This work was funded by the following grants: NIH R01 NS089212, NIH R01 NS074980, and IIT Bombay Seed Grant 14IRCCSG010.

S. Ourselin et al. (Eds.): MICCAI 2016, Part I, LNCS 9900, pp. 237–246, 2016.
DOI: 10.1007/978-3-319-46720-7_28

large number of homologous features across individual cortices [11,12,20]. While the major sulcal patterns are similar across individuals, there is a large individual variation in the folding pattern and, thus, the homology between cortical surfaces of two brains is only approximate. This *partial homology* between two cortices can lead to large within-group variance of cortical properties, e.g., bending, shape, or thickness. Moreover, fine-scale misregistrations, either because of partial homology or numerical challenges in finding the global optimum underlying nonlinear diffeomorphic registration, can lead to invalid between-group comparisons of cortical structure at non-homologous locations.

This paper proposes a novel *statistical descriptor of local cortical geometry* that increases robustness to partial homology and misregistration. The proposed descriptor for cortical folding, and thickness, can lead to easier interpretation, unlike descriptors based on spherical harmonics or spherical wavelets [21]. The proposed descriptor lies on a Riemannian manifold and, unlike related studies on region-based cortical folding [1], uses a method for *hypothesis testing on the Riemannian manifold*.

This paper presents a framework for cross-sectional cortical studies, which models the geometry of the entire cortical sheet, unlike approaches that model either cortical folding or thickness. It proposes a neighborhood-based histogram feature of local cortical shape, which is robust to partial homology and misregistration. It presents a method for hypothesis testing for cross-sectional studies on the Riemannian manifold of histograms. The cross-sectional studies on simulated and clinical brain MRI show the benefits of (i) modeling the entire geometry of the cortex, (ii) the robust histogram-based measure, and (iii) Riemannian hypothesis testing, *each of which* leads to the detection of the between-group differences with greater accuracy and precision.

2 Methods

This section describes the proposed model for the cortical sheet, the robust descriptor of local cortical geometry, and its use for hypothesis testing on a Riemannian manifold.

2.1 Modeling the Cortex

We propose a medial surface model for the cortex, which subsumes models for cortical folding and thickness. The proposed model comprises (i) the mid cortical surface, as the medial surface, and (ii) local cortical thickness values at each point on the mid-cortical surface. Given the mid-cortical surface $\mathcal{M}$, the value of the thickness t at each point m on $\mathcal{M}$ gives the locations of the inner and outer (pial) cortical surfaces, at distances $t/2$ along the inward and outward normals to the mid-cortical surface at m.

We compute cortical thickness based on [7]. We model the geometry of the mid-cortical surface $\mathcal{M}$ through the local surface-patch characteristics at each point on the surface. At every point $m \in \mathcal{M}$, the principal curvatures $\kappa_{\min}(m)$

and $\kappa_{\max}(m)$ describe the local geometry [3] (up to second order and up to a translation and rotation). The space ($\kappa_{\min}(m)$,$\kappa_{\max}(m)$) can be reparametrized, by a polar transformation, into the orthogonal bases of curvedness $C(m) := [\kappa_{\min}(m)^2 + \kappa_{\max}(m)^2]^{0.5}$ and shape index $S(m) := \frac{1}{\pi} \arctan \left[\frac{\kappa_{\min}(m)+\kappa_{\max}(m)}{\kappa_{\min}(m)-\kappa_{\max}(m)}\right]$, which meaningfully separate notions of bending and shape [9], leading to easier interpretation. The shape index $S(m) \in [-1, 1]$ is a pure measure of shape, modulo size, location, and pose. The curvedness $C(m) \geq 0$ captures a notion of surface bending at a particular patch scale/size, and is invariant to location and pose. We compute principal curvatures at m by fitting a quadratic patch to the local surface around m [3].

2.2 Multivariate Local Descriptor of Cortical Folding and Thickness

We propose a novel local descriptor of the cortical geometry (folding as well as thickness) for cross-sectional studies for detecting cortical differences. The partial homology across different brains, biologically limited to about two dozen landmarks in each hemisphere [20], casts doubts on the validity of typical comparisons across non-homologous locations. At location m on the mid-cortical surface in *normalized* space, the partial homology can greatly increase the variance of shape-index values $S_i(m)$ across individuals i. The variance increase reduces the power of the subsequent hypothesis tests.

Surface based smoothing of the shape-index values $S_i(n)$, over a neighborhood of location m, cannot address the partial-homology problem. When the average of the shape index over sulci and gyri leads to a value close to zero, this average is non-informative about the nature of the folding; e.g., the sinusoidal surfaces $f_1(x, y) := \sin(x + y)$ and $f_2(x, y) := \sin(y)$ can both lead to the same average close to zero in sufficiently large neighborhoods. Thus, spatial smoothing of shape-index in leads to (i) high variance at fine scales (as for pointwise analyses) and (ii) loss of differentiability between surfaces at coarse scales (i.e., large neighborhoods). So, a single-/multiscale analysis with shape-index values can be an unreliable indicator of folding differences.

We propose to consider the histogram of shape-index values $S(n)$ in a spatial neighborhood around location n as the feature. The size of the neighborhood for building this histogram depends on the typical size of *regions* (*not* individual points) in the cortex over which sulcal/gyral homologies can be reliably established. This histogram is immune to the inevitable misregistration of sulci/gyri at fine scales. Moreover, unlike the neighborhood average that is a scalar, the histogram is a far richer descriptor that retains neighborhood information by restricting averaging to each histogram bin.

The limitations exhibited by the shape index, because of partial homology, are also shared by the curvedness because the surface path from the crown of a gyrus to a fundus of an adjacent sulcus takes the curvature through a large variation, i.e., from a large positive value to zero (at the inflection point) and back to a large positive value. Cortical thickness appears to be the least affected by the partial homology because thickness exhibits a much smaller variation from gyrus

to sulcus. Nevertheless, because the crowns of gyri are typically 20 % thicker than the fundi of sulci [4], even thickness studies, relying on normalization and groupwise comparison of spatially-averaged thickness values (at multiple scales), suffer from problems related to increased variance/information loss. Thus, we also include curvedness and thickness through their local histograms.

Finally, motivated by the empirically found biological correlations between the values of shape index $S_i(n)$, curvedness $C_i(n)$, and thickness $T_i(n)$, we propose their *joint histogram*, denoted by $H_i(m)$, in the spatial neighborhood (about 5 mm radius) of location m on the medial (mid-cortical) surface, as the local descriptor of the cortex.

2.3 Riemannian Statistical Modeling

We perform hypothesis testing using the joint histograms $H_i(m)$ as the local feature descriptor for the cortex at location m for subject i. If the number of bins in the histogram is B, then $H_i(m) \in (\mathbb{R}_{\geq 0})^B$, $||H_i(m)||_1 = 1$, and $H_i(m)$ lies on a Riemannian manifold. To measure distance between histograms $H_1(m)$ and $H_2(m)$, we use the Fisher-Rao distance metric $d(H_1(m), H_2(m)) := d_g(F_1(m), F_2(m))$, where $F_i(m)$ is the square-root histogram that is denoted $\sqrt{H_i(m)}$, with the value in the b-th bin $F_i(m,b) := \sqrt{H_i(m,b)}$ and $d_g(F_1(m), F_2(m))$ is the geodesic distance between $F_1(m)$ and $F_2(m)$ on the unit hypersphere $\mathbb{S}^{B-1}$ [19].

Modeling a probability density function (PDF) on a hypersphere entails fundamental trade-offs between model generality and the viability of the underlying parameter estimation. For instance, although Fisher-Bingham PDFs on $\mathbb{S}^d$ are able to model generic anisotropic distributions using $O(d^2)$ parameters, their parameter estimation may be intractable [14]. In contrast, parameter estimation for the $O(d)$-parameter von Mises-Fisher PDF is tractable, but that PDF can only model isotropic distributions. We use a tractable approximation of a Normal law on a Riemannian manifold [17], modeling anisotropy through its covariance parameter in the tangent space at the mean.

For a group with I subjects, at each cortical location m, we fit the approximate Normal law to the data $\{\sqrt{H_i(m)}\}_{i=1}^I$ as follows. We optimize for the Frechet mean $\mu \in \mathbb{S}^{B-1}$ via iterative gradient descent on the manifold $\mathbb{S}^{B-1}$ [2], where

$$\mu := \arg\min_{\nu} \sum_{i=1}^{I} d_g^2(\nu, \sqrt{H_i(n)}) \text{ under the constraint } \nu \in \mathbb{S}^{B-1}. \tag{1}$$

We use the logarithmic map $\text{Log}_\mu(\cdot)$ to map the square-root histograms $\{\sqrt{H_i(m)}\}_{i=1}^I$ to the tangent space at the estimated Frechet mean μ and find the optimal covariance matrix Σ in closed form [5]. For any histogram H, we define the squared geodesic Mahalanobis distance between $\sqrt{H}$ and mean μ, given covariance Σ, as $d_M^2(\sqrt{H}; \mu, \Sigma) := \text{Log}_\mu(\sqrt{H})^T \Sigma^{-1} \text{Log}_\mu(\sqrt{H})$. Then, the proposed PDF evaluated at histogram H is

$$P(H|\mu,\Sigma) := \exp\left(-0.5 d_M^2(\sqrt{H};\mu,\Sigma)\right) / ((2\pi)^{(B-1)/2}|\Sigma|^{1/2}). \quad (2)$$

2.4 Permutation Testing for Riemannian Statistical Analysis

Voxel-wise parametric hypothesis testing in the framework of general linear models runs a test at each voxel and adjusts p-values to control for Type-I error arising from multiple comparisons, using Gaussian field theory. However, such parametric approaches make strong assumptions on the data distributions and the dependencies within neighborhoods [15]. In contrast, permutation tests are non-parametric, rely on the generic assumption of exchangeability, lead to stronger control over Type-1 error, are more robust to deviations of the data and effects of processing from an assumed model, and yield multiple-comparison adjusted p values [15].

For permutation testing within the Riemannian manifold of histograms, we use a test statistic for cross-sectional studies to measure the differences between the histogram distributions arising from two cohorts X and Y, at every location m on the cortex. At each cortical location m, for both cohorts $\{H_i^X(m)\}_{i=1}^I$ and $\{H_j^Y(m)\}_{j=1}^J$, we fit the above Riemannian model to estimate the Frechet means $\mu^X(m), \mu^Y(m)$ and covariances $\Sigma^X(m), \Sigma^Y(m)$ (in the respective mean's tangent space). The Hotelling's T^2 test statistic used in the standard multivariate Gaussian case cannot be applied in our Riemannian case because the covariances $\Sigma^X(m)$ and $\Sigma^Y(m)$ are defined in two different (tangent) spaces. Thus, we propose the following test statistic $t(m)$ to measure the dissimilarity between the two cohort distributions by adding the squared Mahalanobis geodesic distance between the group means with respect to each group covariance, i.e.,

$$t(m) := d_M^2(\mu^X(m); \mu^Y(m), \Sigma^Y(m)) + d_M^2(\mu^Y(m); \mu^X(m), \Sigma^X(m)). \quad (3)$$

3 Results and Conclusion

We evaluate the proposed framework on MRI volumes from the OASIS dataset [13]. We use BrainSuite (brainsuite.org) for tissue segmentation, mid-cortical surface extraction, computing thickness and curvature measures, and spatial normalization [8].

Validation on Brain MRI by Simulating Cortical Differences. We randomly assigned 140 control subjects to 2 groups of 50 and 90 subjects. We treat the larger group as normal. For the 50 subjects, we simulated both cortical thinning (eroding the cortex segmentation) and flattening (smoothing the cortex segmentation) in part of the right parietal lobe (Fig. 1(d)). This (i) reduced thickness and curvedness values and (ii) increased the concentration of shape index values around ± 0.5 (corresponding to gyral ridges and sulcal valleys) by smoothing fine-scale cortical features. We then tested for differences between cortices of these 2 cohorts.

The new approach using the *joint histogram* descriptor with Riemannian modeling and hypothesis testing (Fig. 2(d)) correctly shows significantly low p

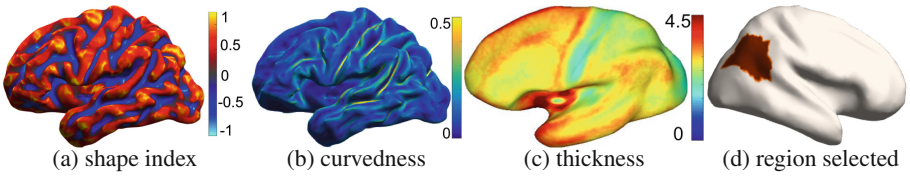

Fig. 1. Cortex parametrization: a sample brain showing computed values of the (a) shape index, (b) curvedness, and (c) thickness, at each point on the mid-cortical surface. **Simulating cortical differences:** (d) Selected region for simulating cortical thinning and flattening.

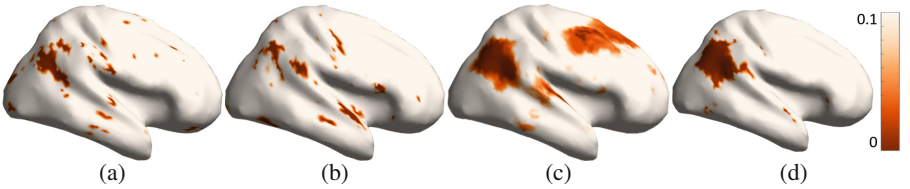

Fig. 2. Validation with simulated differences. Permutation test p values using *Riemannian statistical modeling and hypothesis testing for histogram descriptors* with: (a) shape index, (b) curvedness, (c) thickness, and (d) shape index, curvedness, and thickness *jointly* **(proposed).**

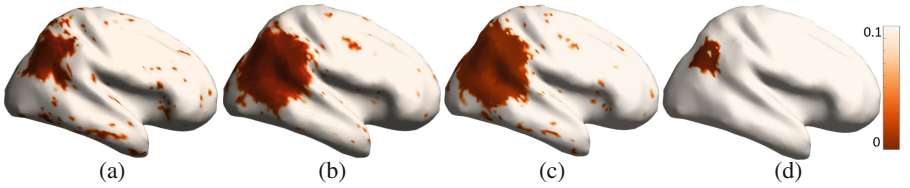

Fig. 3. Validation with simulated differences. Permutation test p values using *multiscale* features of (a) curvedness, (b) thickness, and (c) shape index, curvedness, and thickness jointly. Permutation test p values with the (d) *histogram descriptor and Euclidean statistics.*

values in the thinned-flattened region (Fig. 1(d)) and high p values elsewhere. In contrast, Riemannian analysis on the *marginal* histograms for the shape index (Fig. 2(a)), curvedness (Fig. 2(b)), and thickness (Fig. 2(c)) produces far more Type-I/Type-II errors.

In comparison, a multiscale shape-index descriptor using a Laplacian scale-space pyramid was unable to detect any significant differences (all p values > 0.3; hence, figure *not* shown), multiscale descriptors of curvedness (Fig. 3(a)), thickness (Fig. 3(b)), and joint shape-curvedness-thickness (Fig. 3(c)) lead to a large number of false positives. Furthermore, the *joint histogram* descriptor with Euclidean statistical modeling and hypothesis testing (permutation test with

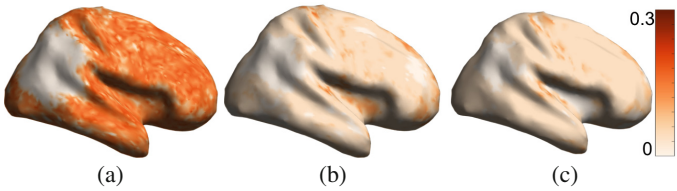

Fig. 4. Simulated differences, stability analysis. *Standard deviation* of permutation test p values, using *bootstrap sampling*, for (a) joint multiscale descriptor, (b) joint histogram descriptor with Euclidean analysis, (c) joint histogram descriptor with Riemannian analysis (**proposed**).

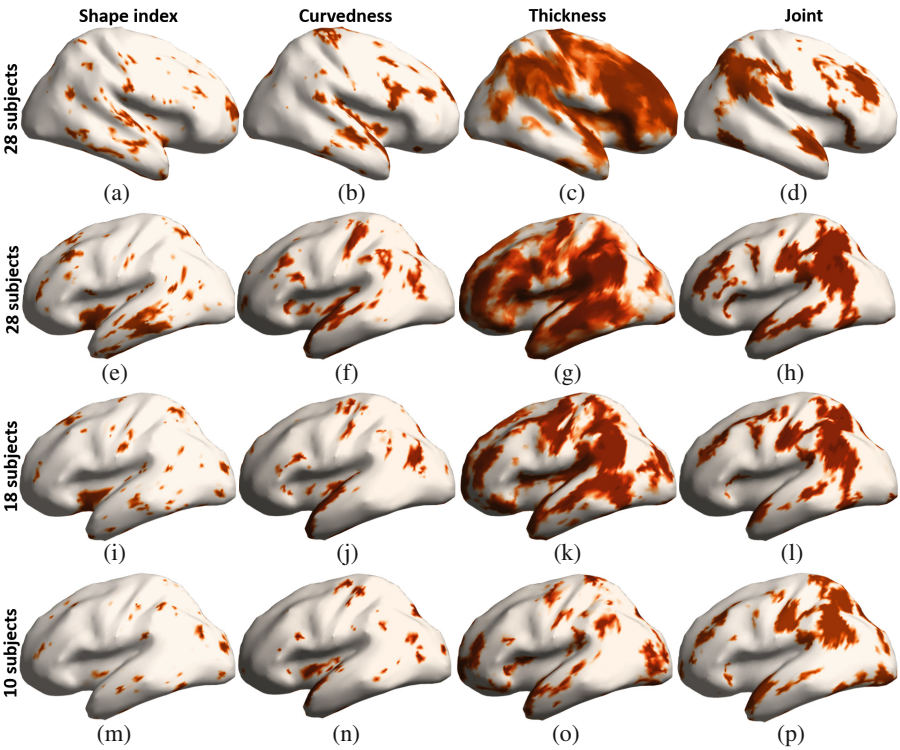

Fig. 5. OASIS, histogram descriptors, Riemannian analysis. Permutation test p values comparing MCI with controls using *Riemannian statistical modeling and hypothesis testing for histogram descriptors*, for both hemispheres, using: (a),(e) shape index, (b),(f) curvedness, (c),(g) thickness, and (d),(h) shape index, curvedness, and thickness *jointly* (**proposed**). Analogous p values with (i)–(l) MCI cohort subset of 18 (randomly chosen) subjects and (m)–(p) MCI cohort subset of the remaining 10 subjects. [Color bar same as Fig. 2]

Hotelling's test statistic) leads to a large number of false negatives (differences detected in shrunk region; Fig. 3(d)).

To evaluate the stability of the p values under variation in cohorts, we computed a set of p values by bootstrap sampling the original cohort. This analysis indicates that the stability of the p values from our framework (Fig. 4(c)) is superior to approaches using (i) multiscale descriptors (Fig. 4(a)) and (ii) histogram descriptors without Riemannian analysis (Fig. 4(b)). The lower values in the parietal lobe are consistent with the location of the selected region where strong differences are introduced.

Comparisons of an MCI Cohort to the Control Group. We tested for differences in 2 cohorts from the OASIS dataset: (i) 140 control subjects and (ii) 28 subjects with mild cognitive impairment (MCI) with a clinical dementia rating of 1. The results using the proposed approach for 28 MCI subjects (Fig. 5(d)) remain far more stable for smaller cohort sizes, i.e., 18 MCI subjects (Fig. 5(l)) and 10 MCI subjects (Fig. 5(p)), as compared to using the histogram descriptors separately for the shape index (Fig. 5(a),(i),(m)), curvedness (Fig. 5(b),(j),(n)), and thickness (Fig. 5(c),(k),(o)). The joint multiscale descriptor (Fig. 6) also leads to widely varying results with change in cohort size. Bootstrap sampling of the cohorts shows that the stability of the p values from our framework (Fig. 7(c)–(d)) are clearly more stable than those using the joint multiscale descriptor (Fig. 7(a)–(b)). Our thickness-based results (Fig. 5(c),(g)) share some similarity with the thickness changes found in MCI [18].

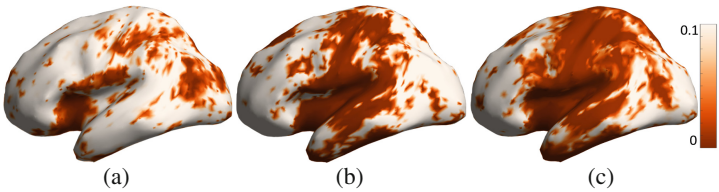

Fig. 6. OASIS, multiscale descriptor. Permutation test p values with the joint multiscale descriptor for a MCI cohort of (a) 10 subjects, (b) 18 subjects, and (c) 28 subjects.

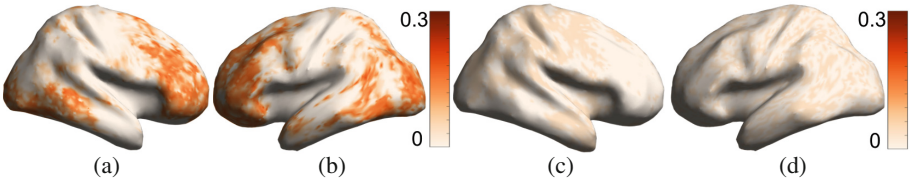

Fig. 7. OASIS, stability analysis. *Standard deviation* of permutation test p values, using *bootstrap sampling* for (a)–(b) joint multiscale descriptor (both hemispheres) and (c)–(d) joint histogram descriptor with Riemannian analysis (both hemispheres) (**proposed**).

Conclusion. We have described a framework for analysis of cortical geometry that combines a novel histogram-based descriptor, which is robust to partial homologies and misregistration, with statistical analysis of a Riemannian manifold. Our results show improved accuracy relative to multiscale approaches in simulations and improved robustness to small sample sizes using clinical data.

References

1. Awate, S., Yushkevich, P., Song, Z., Licht, D., Gee, J.: Cerebral cortical folding analysis with multivariate modeling and testing: studies on gender differences and neonatal development. NeuroImage **53**(2), 450–459 (2010)
2. Buss, S., Fillmore, J.: Spherical averages and applications to spherical splines and interpolation. ACM Trans. Graph. **20**(2), 95–126 (2001)
3. Carmo, M.D.: Differential Geometry of Curves and Surfaces. Prentice Hall, Upper Saddle River (1976)
4. Fischl, B., Dale, A.: Measuring the thickness of the human cerebral cortex from magnetic resonance images. Proc. Nat. Acad. Sci. **97**(20), 11050–11055 (2000)
5. Fletcher, T., Lu, C., Pizer, S., Joshi, S.: Principal geodesic analysis for the study of nonlinear statistics of shape. IEEE Trans. Med. Imaging **23**(8), 995–1005 (2004)
6. Hardan, A., Muddasani, S., Vemulapalli, M., Keshavan, M., Minshew, N.: An MRI study of increased cortical thickness in autism. Am. J. Psychiart. **163**(7), 1290–1292 (2006)
7. Jones, S., Buchbinder, B., Aharon, I.: Three-dimensional mapping of cortical thickness using Laplace's equation. Hum. Brain Mapp. **11**(1), 12–32 (2000)
8. Joshi, A.A., Shattuck, D.W., Leahy, R.M.: A method for automated cortical surface registration and labeling. In: Dawant, B.M., Christensen, G.E., Fitzpatrick, J.M., Rueckert, D. (eds.) WBIR 2012. LNCS, vol. 7359, pp. 180–189. Springer, Heidelberg (2012)
9. Koenderink, J.J.: Solid Shape. MIT Press, Cambridge (1991)
10. Luders, E., Narr, K., Thompson, P., Rex, D., Woods, R., Jancke, L., Toga, A.: Gender effects on cortical thickness and the influence of scaling. Hum. Brain Mapp. **27**, 314–324 (2006)
11. Lyttelton, O., Boucher, M., Robbins, S., Evans, A.: An unbiased iterative group registration template for cortical surface analysis. NeuroImage **34**, 1535–1544 (2007)
12. Mangin, J., Riviere, D., Cachia, A., Duchesnay, E., Cointepas, Y., Papadopoulos-Orfanos, D., Scifo, P., Ochiai, T., Brunelle, F., Regis, J.: A framework to study the cortical folding patterns. NeuroImage **23**(1), S129–S138 (2004)
13. Marcus, D., Wang, T., Parker, J., Csernansky, J., Morris, J., Buckner, R.: Open access series of imaging studies (OASIS): cross-sectional MRI data in young, middle aged, nondemented, and demented older adults. J. Cogn. Neurosci. **19**(9), 1498–1507 (2007)
14. Mardia, K., Jupp, P.: Directional Statistics. Wiley, Hoboken (2000)
15. Nichols, T., Holmes, A.: Nonparametric permutation tests for functional neuroimaging: a primer with examples. Hum. Brain Mapp. **15**(1), 1–25 (2002)
16. Nordahl, C., Dierker, D., Mostafavi, I., Schumann, C., Rivera, S., Amaral, D., Van-Essen, D.: Cortical folding abnormalities in autism revealed by surface-based morphometry. J. Neurosci. **27**(43), 11725–11735 (2007)

17. Pennec, X.: Intrinsic statistics on Riemannian manifolds: basic tools for geometric measurements. J. Math. Imaging Vis. **25**(1), 127–154 (2006)
18. Redolfi, A., Manset, D., Barkhof, F., Wahlund, L., Glatard, T., Mangin, J.F., Frisoni, G.: Head-to-head comparison of two popular cortical thickness extraction algorithms: a cross-sectional and longitudinal study. PLoS ONE **10**(3), e0117692 (2015)
19. Srivastava, A., Jermyn, I., Joshi, S.: Riemannian analysis of probability density functions with applications in vision. In: Proceedings of International Conference on Computer Vision and Pattern Recognition, pp. 1–8 (2007)
20. Van-Essen, D., Dierker, D.: Surface-based and probabilistic atlases of primate cerebral cortex. Neuron **56**, 209–225 (2007)
21. Yeo, B.T.T., Yu, P., Grant, P.E., Fischl, B., Golland, P.: Shape analysis with overcomplete spherical wavelets. In: Metaxas, D., Axel, L., Fichtinger, G., Székely, G. (eds.) MICCAI 2008, Part I. LNCS, vol. 5241, pp. 468–476. Springer, Heidelberg (2008)
22. Yu, P., Grant, P., Qi, Y., Han, X., Segonne, F., Pienaar, R., Busa, E., Pacheco, J., Makris, N., Buckner, R., Golland, P., Fischl, B.: Cortical surface shape analysis based on spherical wavelets. IEEE Trans. Med. Imaging **26**(4), 582–597 (2007)